

A parametric study of indicial function models in bridge deck aeroelasticity

C. Borri[†] and C. Costa[‡]

CRIACIV⁽¹⁾, Dipartimento di Ingegneria Civile, Università degli Studi di Firenze, Firenze, Italy
(Received December 31, 2003, Revised July 1, 2004, Accepted August 30, 2004)

Abstract. In common approaches, bridge dynamics under wind action is analyzed by modeling the interaction between fluid and structure by means of transient wind loads acting over the structure itself. Amid various possible manners to describe such types of loads, a representation based on families of 'indicial functions' is adopted here. The aim is to investigate its flexibility to capture the main features of wind-bridge interaction. A set of coefficients is involved in indicial functions. The values that one may attribute to them suffer uncertainties coming from experimental errors affecting data. Here, the sensitivity of a 2-DOF schematic model to the variations of these coefficients is investigated at fixed values of dynamic derivatives and for various types of indicial functions. It is shown how parameter variations influence phase portraits.

Keywords: aeroelasticity; bridges; time-domain simulations; indicial functions.

1. Introduction

The description of the aerodynamic behavior of bridges under wind action is a challenging problem in structural engineering. One needs to describe the interaction between bridge and atmospheric boundary layer in turbulent regime in order to evaluate critical phenomena like flutter and vortex-induced vibrations. A way to tackle the problem is to put the attention on the bridge itself and to describe the action over it (exerted by the fluid) by means of transient wind loads. If this approach is followed, the basic problem is a realistic model of such loads, once a structural scheme of the bridge is selected.

Often, a two-dimensional framework is used and just the behavior of the typical cross-section of the bridge is described. In this case, to represent transient loads induced by wind action, several methods can be applied. They are frequency-based or time domain techniques. In particular, time domain approaches seem to be convenient to represent non-stationary behavior of bridges in turbulent flow because they allow one to account for all prominent non-linearities (in contrast with frequency-based approaches) even if, strictly speaking, the load model remains linearized. However, standard time domain methods used in aerodynamics to describe the behavior of wing profiles cannot be applied directly and require adjustments: in fact, the cross-section of a bridge does not coincide typically with an airfoil embedded in a perfect flow.

[†] Full Professor, Dr.-ing. h. c.

[‡] Ph. D., Dr.-ing., M.I.T. Fellow 2003

⁽¹⁾Centro di Ricerca Interuniversitario di Aerodinamica delle Costruzioni e Ingegneria del Vento

Various proposals about appropriate extensions of time domain methods are discussed in literature since the pioneer work of Scanlan, B eliveau and Budlong (1974). In general, the starting point relies upon Fung's theoretical representation of aeroelastic forces for the thin airfoil (Fung 1968) where the circulatory or transient part of the wind action is modeled by using *downwash* w and Wagner's function ϕ (Wagner 1925). The latter is an *indicial* function, where the word 'indicial' refers to a quantity arising from an abrupt change in the state of the system. In particular, Wagner's function describes the lift on a thin airfoil as a consequence of a sudden variation in the angle between the prevalent direction of the wind and the main characteristic linear dimension of the airfoil (*angle of attack*). Up to a certain extent, Fung's representation of wind action can be extended to objects different from airfoils by simply selecting special indicial functions. Moreover, more than one indicial function can be used in order to separate the effects of the different degrees of freedom on the force components (see Bisplinghoff, *et al.* 1996). In this way a comparison with the standard aeroelastic derivative model proposed by Scanlan and Tomko (1971) (in which wind action is expressed by means of frequency-dependent quantities) can be developed.

In the two-dimensional setting of cross-section models, stochastic effects induced by turbulence may be accounted for as proposed by Lin and Li (1993). Furthermore, the unsteady behavior of the bridge taking into account the fading memory of the fluid enveloping the body (Borri and Hoeffler 2000) can be modeled in the context of a finite element analysis, for example by means of the integration scheme proposed by Borri, *et al.* (2002).

Indicial functions are characterized by certain coefficients whose values are usually obtained by calibration on experimental data. Usually, the method applied is a standard interpolation of data based on minimization of the error by using non-linear least square procedures (Scanlan, *et al.* 1974, Borri and Hoeffler 2000, Caracoglia and Jones 2003). The difference between the indicial functions obtained by transient vibration tests and the corresponding functions derived in tests affected by ambient vibrations is discussed by Zhang, *et al.* (2003): they point out in some way an influence of the oscillation amplitude on the transfer functions. Bucher and Lin (1989) propose an approximation of the aeroelastic derivatives by using a series of rational functions independent of frequency, by following the operational treatment of Jones (1938). An analogous approach is followed also by Ding and Lee, for an analysis of the buffeting response (Ding and Lee 2000), by Boonyapinyo, *et al.* (1999) and by Chen, *et al.* (2000), where coupling with a finite element method allows one to simulate the motion of a bridge in turbulent flow.

In this paper, a model with unsteady transient wind loads modeled through indicial functions is considered: such functions have the advantage of being interpretable as physically meaningful quantities and treatable with Fourier transform because of their exponential form.

A parametric analysis on selected dynamic systems is then performed in phase space at given values of aerodynamic coefficients, to evaluate the sensitivity of the model to uncertainties arising from experimental data. It is shown that the influence of uncertainties on indicial function coefficients affects mainly the oscillation amplitude. The influence is different in intensity for each indicial function. In the cases analyzed, the main effect is due to the y -lift indicial function, that affects also the stability of the system. Such a circumstance is due to the streamlined geometry of the section taken into account in numerical examples, which is a typical shape of suspension bridges. The method can be analogously applied to sections with different and more bluff geometries, in particular expecting a major role of the indicial functions related to the aerodynamic moment. Extreme cases are presented, to quantify the importance of the different functions by

means of the determination of upper and lower bounds. Results of the previous analyses are confirmed, suggesting a prominent role of the lift function on the coupled flutter mechanism.

The results obtained here furnish first information on the qualitative behavior of the dynamic system describing wind-bridge interaction. Further numerical examples can be developed. They should involve variations in the aerodynamic coefficients and sectional geometry and will be presented in a forthcoming work.

2. Mechanical model

The attention is focused on a bridge cross-section. The structural scheme adopted is an elementary two-dimensional model simulating the behavior of an elementary strip of a bridge deck in a wind flow (Fig. 1(a)).

The main characteristic dimension is assumed to be the width of the deck section B , referred to as the *chord*. Half of the chord is indicated with $b=B/2$. The thickness of the section is indicated with D , the span of the bridge with l . The ratio B/D between the chord and the thickness is a parameter used to describe the slenderness of the structure.

The cross-section is studied as a rigid body, suspended by means of springs with translational stiffness k , coupled with dampers, with damping constants c , fixed at a certain distance d from the elastic center E . The pairs spring-damper give to the section a vertical stiffness $k_y=2k$, a torsional stiffness $k_\alpha=2d^2k$, a vertical damping $c_y=2c$ and a torsional damping $c_\alpha=2d^2c$. The section has mass m and mass moment of inertia I per unit span.

The section is symmetric, with respect to the chord and to the vertical axis. The center of mass G is then placed at the intersection of the symmetry axes. The elastic center E is coincident with the center of mass. They are both located at the midspan of the deck section.

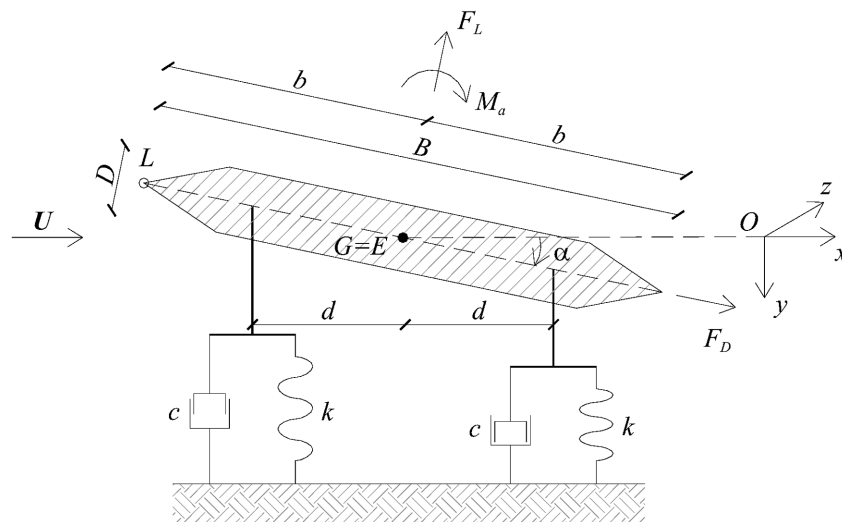


Fig. 1(a) Characteristics of the bridge deck section (B = chord; b = half-chord; D = thickness; k = stiffness constant; c = damping constant; d = distance between restraints and elastic center); relevant points (G = center of mass; E = elastic center; L = leading edge); wind forces (F_L = lift force; F_D = drag force; M_a = aerodynamic moment); wind flow (U = wind velocity); reference system ($Oxyz$)

The first point invested conventionally by the flow is the leading edge L .

The axes of the global reference system $Oxyz$ are the horizontal x , positive downwind and the vertical y , positive downwards. Positive rotations are assumed clockwise.

The degrees of freedom of the model are the vertical displacement y and the rotation α about the center of mass. The wind flow is horizontal and laminar, its velocity is indicated with U .

The motion of the 2-DOFs model is ruled by the balance equations

$$\begin{cases} m\ddot{y} + c_y\dot{y} + k_y y = F_y(t) \\ I\ddot{\alpha} + c_\alpha\dot{\alpha} + k_\alpha\alpha = M_a(t) \end{cases} \quad (1)$$

where F_y and M_a represent the self-excited vertical force and moment due to wind-structure interaction. The vertical force F_y depends on lift force F_L , acting in the normal direction, and drag force F_D , applying in the direction parallel to the section at each instant. All quantities in Eq. (1) are functions of time t . The dot denotes differentiation with respect to time t .

It is useful to consider an analogous system, where all the terms are expressed as functions of dimensionless time s , as common in aerodynamics. In particular, $s = Ut/b$ (i.e., s is the distance traveled by a wind particle of velocity U , from the time origin, with reference to the deck semi-chord). In terms of s , one obtains

$$\begin{cases} m\frac{U^2}{b^2}y'' + c_y\frac{U}{b}y' + k_y y = F_y(s) \\ I\frac{U^2}{b^2}\alpha'' + c_\alpha\frac{U}{b}\alpha' + k_\alpha\alpha = M_a(s) \end{cases} \quad (2)$$

where primes stand for differentiation with respect to the dimensionless time s .

To solve the system of differential Eqs. in (2), consistent expressions for self-excited forces F_y and M_a need to be assigned: these expressions have the form of dynamic wind pressures modified including relevant displacement and velocity components of the cross-section itself. The appropriate expressions will be discussed in the following.

3. Wind load model: indicial functions

The thin airfoil is analyzed first to set the load scheme, then appropriate modifications are introduced to adapt it to a bridge cross-section.

3.1. The thin airfoil

Some differences in the geometry of a thin airfoil with respect to the symmetric bridge cross-section described in Fig. 1(a) need to be pointed out. In particular, a significant role is played in the airfoil by the rear point R , placed at three-quarter chord distance from the leading edge, and by the aerodynamic center C , at one-quarter distance from the leading edge (see Fig. 1(b)).

The total lift is applied at the point C , because only the lift force arising from circulation is considered, that is all the effects related to added mass are neglected. The center of mass G and the

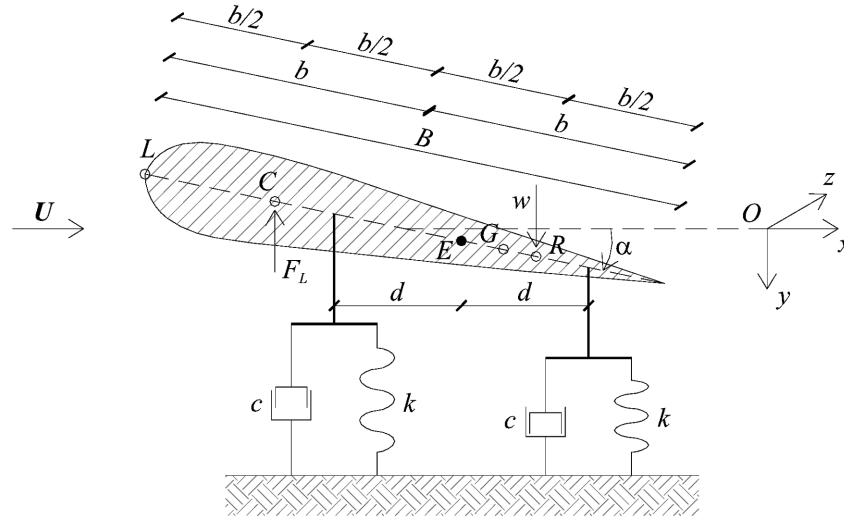


Fig. 1(b) Characteristics of the airfoil (B = chord; b = half-chord; k = stiffness constant; c = damping constant; d = distance between restraints and elastic center); relevant points (C = aerodynamic center; G = center of mass; E = elastic center; L = leading edge); wind forces (F_L = lift force); wind flow (U = wind velocity); w = downwash; reference system ($Oxyz$)

elastic center E are placed somewhere along the chord and are in general not coincident.

The unsteady wind action is modeled with the Wagner's function $\phi(s)$ given, in Jones' approximation (Jones 1939), as function of s :

$$\phi(s) = 1 - 0.165e^{-0.0455s} - 0.335e^{-0.30s} \quad (3)$$

Wagner's function depicts the growth of circulation about the airfoil due to a sudden increase of the downwash w acting at the rear point R , where the downwash is the vertical velocity of the fluid particle in contact with the profile, due to rotational displacement and to rotational and vertical velocities (Fig. 2).

Namely, the function $w(t)$ is given by

$$w(t) = \left[\dot{y}(t) + U\alpha(t) + \frac{b}{2}\dot{\alpha}(t) \right] \quad (4)$$

or, with respect to dimensionless time, by

$$w(s) = \begin{cases} \left[\frac{U}{b}y'(s) + U\alpha(s) + \frac{U}{2}\alpha'(s) \right], & \text{if } s \geq 0 \\ 0, & \text{if } s < 0 \end{cases} \quad (5)$$

The downwash w is positive for a clockwise rotation angle (see the reference frame in Fig. 1(b)). In this case, the positive lift force is assumed upwards, then opposite to the direction of the vertical reference axis y . Lift force F_L should be represented as normal to the airfoil chord, but, as thin airfoil theory is adopted, small angles of attack are assumed and drag forces are absent, giving a

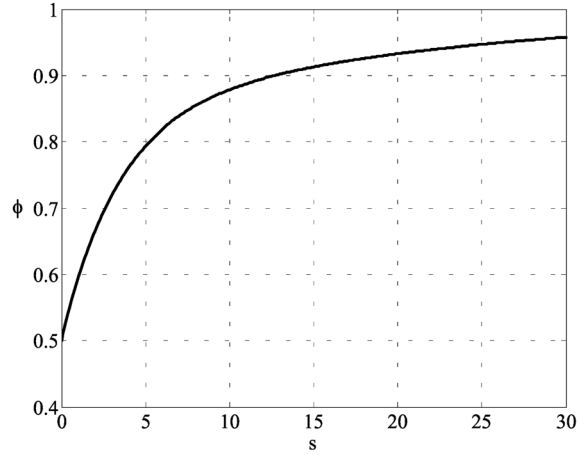


Fig. 2 Wagner's function (Jones' approximation)

resulting vertical lift.

The instantaneous value of the lift force is given by

$$F_L(s) = -2\pi\rho Ubw\phi(s) \quad (6)$$

considering that the net angle of attack corresponds to the ratio of downwash w and horizontal wind speed U .

When a generalized time history of the action is considered, a superposition of elementary lift forces can be accounted for and the total lift force F_L can be written in terms of a convolution integral (Scanlan and Tomko 1971), namely

$$F_L(s) = -2\pi\rho Ub \int_{-\infty}^s \phi(s-\tau)w'(\tau)d\tau \quad (7)$$

with reference to the theoretical aerodynamic coefficient 2π .

One remarks also that $\lim_{s \rightarrow 0^+} w(s) = 0$.

The expression of the lift force F_L can be simplified by integrating by parts. From Eq. (7), it follows that

$$\int_{-\infty}^s \phi(s-\tau)w'(\tau)d\tau = \phi(0)w(s) + \int_{-\infty}^s \phi'(s-\tau)w(\tau)d\tau \quad (8)$$

then, by using the assumptions in Eq. (5), one gets

$$F_L(s) = -2\pi\rho U^2 b^2 \left\{ \left[\frac{y'(s)}{2b} + \frac{\alpha(s)}{2} + \frac{\alpha'(s)}{4} \right] + \int_0^s \phi'(s-\tau) \left[\frac{y'(\tau)}{b} + \alpha(\tau) + \frac{\alpha'(\tau)}{2} \right] d\tau \right\} \quad (9)$$

In the airfoil case, the aerodynamic moment M_a is simply obtained by multiplying F_L by $b/2$, that is by the distance between the application point of the circulation lift C and the midchord:

$$M_a(s) = \pi\rho U^2 b^2 \left\{ \left[\frac{y'(s)}{2b} + \frac{\alpha(s)}{2} + \frac{\alpha'(s)}{4} \right] + \int_0^s \phi'(s-\tau) \left[\frac{y'(\tau)}{b} + \alpha(\tau) + \frac{\alpha'(\tau)}{2} \right] d\tau \right\} \quad (10)$$

The sole contributions included in the aeroelastic forces are therefore those related to the circulatory terms, i.e., the unsteady contributions.

Balance equations reduce then to

$$\begin{cases} y'(s) = u(s) \\ \alpha'(s) = v(s) \\ m \frac{U^2}{b^2} u'(s) + c_y \frac{U}{b} u(s) + k_y y(s) = F_y(s) \\ I \frac{U^2}{b^2} v'(s) + c_\alpha \frac{U}{b} v(s) + k_\alpha \alpha(s) = M_a(s) \end{cases} \quad (11)$$

for an airfoil of unitary length.

3.2. The bridge deck section

The behavior of the bridge deck section can be described by means of a set of balance equations similar to those of the airfoil (11). Of course, such a system captures the prominent features of the mechanical behavior of the bridge cross-section, as much as the section approaches the airfoil profile. In fact, for bluff sections, the hypothesis of fully reattached flow used in the airfoil theory is no more valid and the section itself cannot be considered as immersed in a potential flow. Moreover, the positions of aerodynamic center and rear point are not known. Strictly, no theoretical formulation of the lift force is therefore available for bridge decks. An extension of the theory of the airfoil can nevertheless be formulated to include streamlined and bluff bridge sections in a more complete model. To this aim, appropriate coefficients are defined to well represent the action on the structure.

A family of Wagner-like functions Φ is introduced to model the unsteady wind action:

By following (Fung 1968)

$$\Phi(s) = a_0 - \sum_{j=1}^n a_j e^{-b_j s} \quad (12)$$

where n is the order of the Wagner-like function. Specific numerical values need to be assigned to the a_0 , a_j and b_j coefficients.

Following the formulation of self-excited forces provided by Caracoglia and Jones (2003), the expressions of the lift force and the aerodynamic moment become

$$\begin{aligned} F_L &= \frac{\rho U^2 B}{2} \frac{dC_L(\alpha)}{d\alpha} \Big|_{\bar{\alpha}} \int_{-\infty}^s \left(\Phi_{L\alpha}(s-\tau) \alpha'(\tau) + \Phi_{Ly}(s-\tau) \frac{y''(\tau)}{B/2} \right) d\tau \\ M_a &= \frac{\rho U^2 B^2}{2} \frac{dC_M(\alpha)}{d\alpha} \Big|_{\bar{\alpha}} \int_{-\infty}^s \left(\Phi_{M\alpha}(s-\tau) \alpha'(\tau) + \Phi_{My}(s-\tau) \frac{y''(\tau)}{B/2} \right) d\tau \end{aligned} \quad (13)$$

If the expression of the lift force F_L in Eq. (13) is compared with the expression in Eq. (7), one may observe that the Wagner's function ϕ is substituted with two new functions, that is Φ_{Ly} and $\Phi_{L\alpha}$, and vertical velocity, rotation angle and rotational velocity contributions to the downwash are separated.

Only vertical velocity and rotation angle do appear in Eq. (13), because the contribution of the rotational velocity is neglected, as suggested in Zhang, *et al.* (2003). The indicial functions Φ_{Ly} and $\Phi_{L\alpha}$ describe, respectively, the elementary lift forces associated with a sudden unit variation in vertical velocity and rotation angle.

Analogous description is adopted for the aerodynamic moment M_α , expressed by means of the Φ_{My} and $\Phi_{M\alpha}$ indicial functions.

The two indices of each function Φ identify respectively the relevant force component and the mechanical quantity interested by the sudden change.

The elementary forces are superimposed to obtain the total forces, by means of a convolution integral. The load model is then linear. Moreover, small rotations are accounted for, then the y force F_y can be substituted directly with the lift force F_L . Drag forces are moreover neglected.

The aerodynamic coefficients $dC_L(\alpha)/d\alpha$ and $dC_M(\alpha)/d\alpha$ may vary here, whereas, in the standard airfoil model, they attain the following values: the lift coefficient is $dC_L(\alpha)/d\alpha = 2\pi$, while the moment coefficient is $dC_M(\alpha)/d\alpha = \pi/2$. The variation is however very slight, in the case of small rotations.

This load model can be related to the frequency domain model by means of a Fourier transform: a direct comparison between coefficients of indicial functions and frequency-dependent quantities (aeroelastic derivatives) can be made, obtaining in a closed form the relationships between couples of aeroelastic derivatives and indicial function coefficients (Borri, *et al.* 2002).

In this case, balance equations reduce to:

$$\left\{ \begin{array}{l} y'(s) = u(s) \\ \alpha'(s) = v(s) \\ u'(s) = -\frac{c_y b}{mU} u(s) - \frac{k_y b^2}{mU^2} y(s) - \frac{\rho b^3}{m} \frac{dC_L}{d\alpha} \bigg|_{\bar{\alpha}} \left(\int_0^s \Phi_{L\alpha}(s-\tau) v(\tau) d\tau + \int_0^s \Phi_{Ly}(s-\tau) \frac{u'(\tau)}{b} \right) \\ v'(s) = -\frac{c_\alpha b}{IU} v(s) - \frac{k_\alpha b^2}{IU^2} \alpha(s) + \frac{\rho b^4}{I} \frac{dC_M}{d\alpha} \bigg|_{\bar{\alpha}} \left(\int_0^s \Phi_{M\alpha}(s-\tau) v(\tau) d\tau + \int_0^s \Phi_{My}(s-\tau) \frac{u'(\tau)}{b} \right) \end{array} \right. \quad (14)$$

4. Numerical procedure

The behavior of the bridge cross-section can be described through the system of integro-differential Eqs. (14). A suitable solution method is a fourth-order Runge-Kutta scheme.

The normal form of the system of Eqs. is $p' = f(s, p)$, where $p = [y, \alpha, u, v]$. If an integration by parts following (8) is performed, one obtains a modified system, in which indicial functions and their derivatives with respect to the dimensionless time do appear

$$\left\{ \begin{array}{l} y' = u \\ \alpha' = v \\ u' = f(y, u, v, \Phi, \Phi') \\ v' = g(\alpha, u, v, \Phi, \Phi') \end{array} \right. \quad (15)$$

Table 1 Runge-Kutta scheme for a differential equation of the first order $p' = f(s, p)$

s	p	$k_i = hf_i(s, p)$
s_0	p_0	k_1
$s_0 + h/2$	$p_0 + k_1/2$	k_2
$s_0 + h/2$	$p_0 + k_2/2$	k_3
$s_0 + h$	$p_0 + k_3$	k_4
$s_1 = s_0 + h$	$p_1 = p_0 + k_{step}$	$k_{step} = 1/6(k_1 + 2 k_2 + 2 k_3 + k_4)$

This integro-differential system is discretized along the s -axis. Each time step of amplitude $\Delta s = h$ includes two intermediate intervals $[s, s+h/2]$ and $[s+h/2, s+h]$, and the vector variable p is evaluated at the boundary of each interval. For each time step a constant value k_{step} is evaluated, in order to calculate the upgraded variables. This constant is obtained by considering a weighted sum of intermediate values k_i , following the scheme of Table 1, calculated once assigned the f_i functions.

The evaluation of the convolution integral is performed by means of the rectangular rule, by taking into account all the displacement and velocity histories of the section, since the origin of dimensionless time. The computational effort rapidly increases with the simulation time, because the whole history motion has to be stored and used to evaluate the convolutions. A procedure to consider the fading memory of the system and, at the same time, to reduce the computational effort, is proposed in Borri, *et al.* (2002). The unsteady contribution of each elementary force tends to a quasi-steady value (see Fig. 2) and therefore its effect on the actual time decreases, as integration time increases. It is possible to change the integration limits, considering a moving time window that includes only the last part of the unsteady forces.

In this case the integration step is set up as $\Delta s = h = 0.001$, in order to avoid the aliasing problem and to obtain an accurate solution.

5. Numerical examples

Two numerical examples are analyzed. The first deals with a thin airfoil to test the numerical procedure, while, in the second example, a streamlined bridge deck cross-section is examined, in order to evaluate the contributions of the coefficients of indicial functions.

5.1. The thin airfoil

The geometrical properties of the section are given in Table 2 together with some dynamic data. In addition, the circular frequencies ω_y and ω_α are given.

The dynamic behavior of the section is evaluated and a critical wind velocity, at which the flutter phenomenon occurs, is identified with different methods. This is the typical case of coupled flutter, where the critical frequency attains an intermediate value between the two natural structural frequencies.

The critical wind velocity U_{crit} and the corresponding coupling frequency ω_{crit} are obtained with

Table 2 Characteristics of the airfoil section

$l = 0.45$ m	$b = 0.08$ m	$\omega_y = 8.5$ rad/s	$m = 4.1202$ kg/m	$\zeta_y = 0.0022$
$D = 0.005$ m	$B = 0.16$ m	$\omega_\alpha = 12.8$ rad/s	$I = 0.02031$ kgm ² /m	$\zeta_\alpha = 0.0060$

Table 3 Thin airfoil flutter speed

Flutter analysis method	U_{crit} [m/s]	ω_{crit} [rad/s]	$U_{red, crit}$
Theoretical eigenvalues analysis	7.26	10.46	27.26
Indicial functions numerical simulation	8.10	10.56	30.13
Wind tunnel tests	8.80	11.30	30.58

different methods: i) a theoretical eigenvalues analysis, ii) an indicial function numerical simulation, and compared with that ones experimentally derived in wind tunnel tests (see Falco, *et al.* 1978). Results are provided in Table 3. As a first step, the critical flutter condition is evaluated by means of an eigenvalue analysis for a theoretical flat plate, that is with aerodynamic coefficients $dC_L(\alpha)/d\alpha = 2\pi$, $dC_M(\alpha)/d\alpha = \pi/2$, $C_D = 0.00$, evaluated around zero angle of attack. These theoretical values are compared (see Table 3) with results obtained for the real system, characterized by aerodynamic coefficients $dC_L(\alpha)/d\alpha = 5.73$, $dC_M(\alpha)/d\alpha = 0.943$ and $C_D = 0.10$.

The indicial model (in this case adopting the theoretical Wagner's function but aerodynamic coefficients referred to the real profile) gives an error of 10% in velocity and 9% in frequency, then in good agreement with the experimental results.

5.2. Streamlined bridge deck section

As example, a streamlined symmetric bridge deck section is analyzed, with a $B/D = 12.5$ ratio. Its dynamic behavior is analyzed by varying the coefficients of the indicial functions, analyzing how the value of the parameters can affect influence the motion of the section. Geometric and inertial properties of the section are shown in Table 4.

The chosen indicial function coefficients are referred to the Tsurumi-Fairway bridge cross-section, already studied in Caracoglia and Jones (2003), Sarkar, *et al.* (1994), Scanlan (2000). The following values are assigned to the aerodynamic coefficients: $dC_L(\alpha)/d\alpha = -3.370$, $dC_M(\alpha)/d\alpha = 0.943$.

The values of the indicial function coefficients are recalled in Table 5. The a_0 coefficient is set up

Table 4 Characteristics of the bridge deck section-model

$l = 0.920$ m	$b = 0.1875$ m	$\omega_y = 36.88$ rad/s	$m = 3.738$ kg/m	$\zeta_y = 0.0018$
$D = 0.03$ m	$B = 0.375$ m	$\omega_\alpha = 52.15$ rad/s	$I = 0.03609$ kgm ² /m	$\zeta_\alpha = 0.0028$

Table 5 Tsurumi Fairway Bridge indicial functions coefficients

IF	a_1	b_1				
Φ_{Ly}	3.035	1.316				
	a_2	b_2	a_3	b_3	a_4	b_4
$\Phi_{L\alpha}$	-1.868	1.978	0.784	0.559	-0.334	0.101
	a_5	b_5				
Φ_{My}	0.829	0.348				
	a_6	b_6				
$\Phi_{M\alpha}$	0.305	0.390				

to 1 in every case.

Qualitative analyses in the phase plane and time domain simulations are addressed. To quantify the sensitivity of the motion to the different parameters, a proper interval of variation of such parameters is selected and different analyses are performed. In fact, the experimental quantities that need to be extracted to define the load model can be affected by uncertainties, because of the scaling of the experimental set-up and of the measurement instruments. It is then interesting to have an idea of how and how much a variation in the parameters can affect the solution of the dynamic problem.

In this case, only the variation of indicial function coefficients is accounted for. The influence of the variation of aerodynamic coefficients is not taken into account, at the present stage, considering that only a small variation is expected. Moreover, in the framework of a different load model (Borri Costa 2004), it is shown that a small influence of such parameters can exist, especially in the region of flutter instability.

5.2.1. Parametric analyses

For each coefficient of indicial functions, a variation of 10% around the assigned values is considered. The amplitude $\pm 10\%$ of variation of the coefficients is in accord with the safe evaluation of possible experimental errors.

All the coefficients of the indicial functions are varied in the same interval. Different results arise for different functions.

The indicial function Φ_{Ly} is considered first. This function is described by means of only one exponential group, characterized by the pair of coefficients (a_1, b_1) .

Preliminary analyses are performed with equal velocity of the oncoming flow $U = 8.10$ m/s and following initial conditions assigned on displacements and velocities: [$y_0 = 0.1$ m, $\alpha_0 = 0.1$ rad, $u_0 = 0.1$ m/s, $v_0 = 0.1$ rad/s]. Three different values of the a_1 coefficient are considered, respectively at the bottom, in the center, and at the end of the 10% amplitude interval. In this case, both the amplitude of displacements and stability of the system are affected by the variation of the coefficients.

Precisely, in all three phase portraits, corresponding to the relevant values of the parameter, a regular limit cycle can be identified for the y displacement, with respect to the vertical velocity (Fig. 3), while the plot of the α displacement versus the rotational velocity (Fig. 4) is more irregular. Both the oscillations are divergent. The relationship between the vertical displacement and the rotation is plotted in Fig. 5, evidencing a boundary in the y direction. The variation of Φ_{Ly} coefficients affects particularly the vertical motion. A minor influence is observed on the rotation of the section.

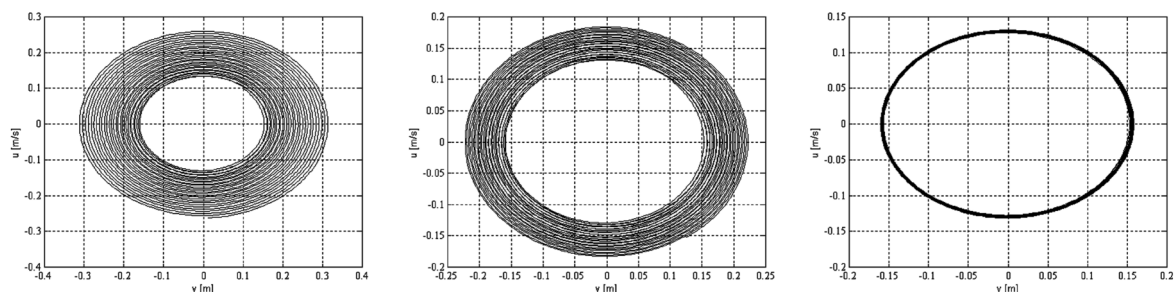


Fig. 3 $y - \dot{y}$ phase diagrams ($1 - a_1(\Phi_{Ly}) = 2.732$, $2 - a_1(\Phi_{Ly}) = 3.035$, $3 - a_1(\Phi_{Ly}) = 3.339$)

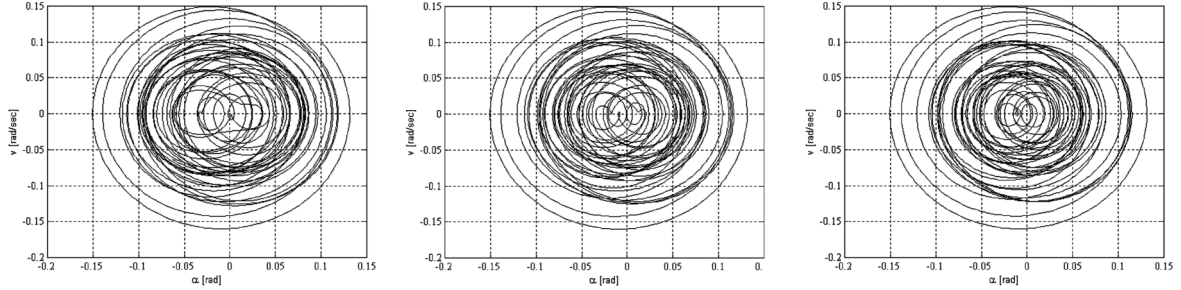


Fig. 4 $\alpha - \dot{\alpha}$ phase diagrams ($1-a_1(\Phi_{Ly}) = 2.732, 2-a_1(\Phi_{Ly}) = 3.035, 3-a_1(\Phi_{Ly}) = 3.339$)

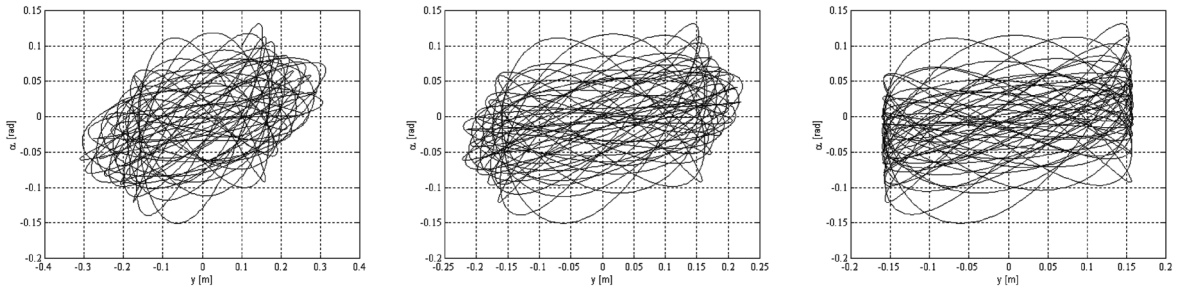


Fig. 5 $y - \alpha$ phase diagrams ($1-a_1(\Phi_{Ly}) = 2.732, 2-a_1(\Phi_{Ly}) = 3.035, 3-a_1(\Phi_{Ly}) = 3.339$)

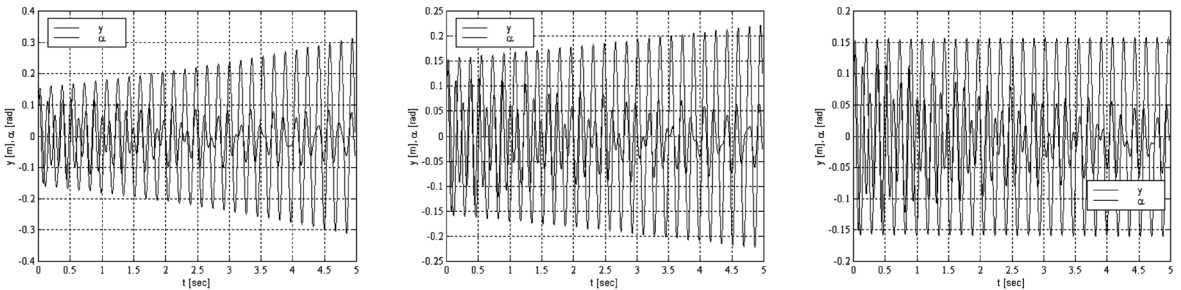


Fig. 6 Time evolution of system ($1-a_1(\Phi_{Ly}) = 2.732, 2-a_1(\Phi_{Ly}) = 3.035, 3-a_1(\Phi_{Ly}) = 3.339$)

In Fig. 6, the time domain plots evidence that a $\pm 10\%$ variation of the a_1 coefficient gives rise to both a diverging and a decaying motion.

In the same manner, three different values of the b_1 coefficient are considered, respectively at the bottom, in the center and at the end of the 10% amplitude interval. Also in this case, the amplitude of displacements and the stability of the system are affected by the variation of the parameter (Fig. 7).

A more refined analysis, utilizing more than three values of the parameter of interest (in this case a_1 and b_1), is performed, to follow the amplitude reached by the two DOFs and to evidence the corresponding relationships parameter-amplitude, in particular their linear or non-linear nature.

The main information obtained is again that the oscillation amplitude is strongly influenced by the values of a_1 and b_1 coefficients: in Fig. 8(a) and Fig. 8(b), the amplitude of the two DOFs is normalized with respect to the maximum of the displacement occurring at the first cycle of

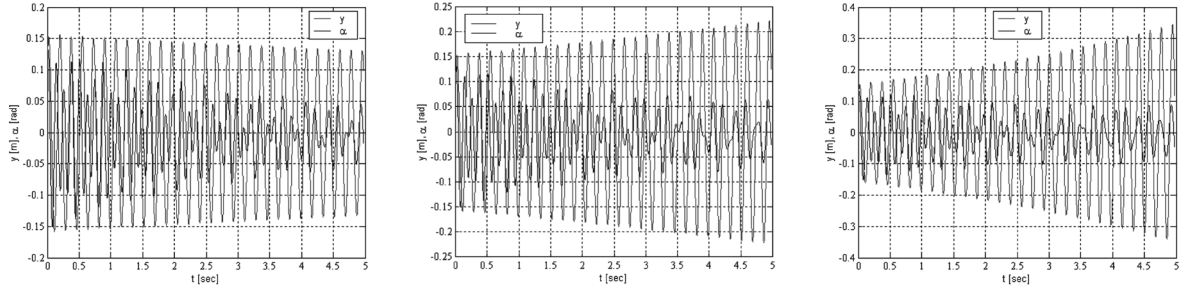
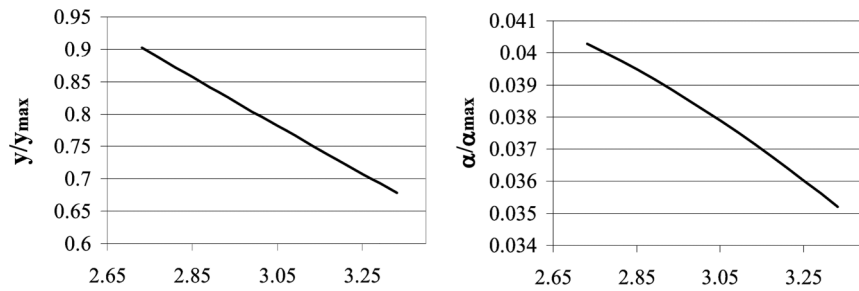
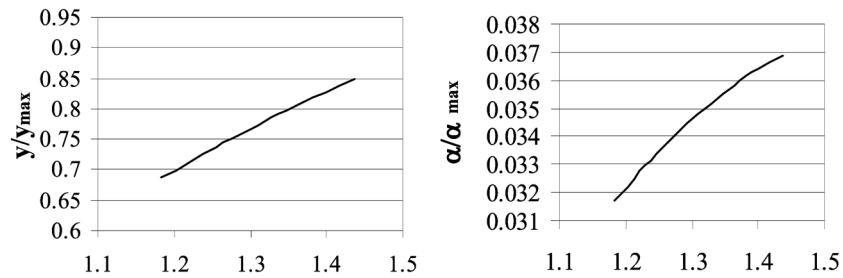


Fig. 7 Time evolution of system ($1-b_1(\Phi_{Ly}) = 1.184$, $2-b_1(\Phi_{Ly}) = 1.316$, $3-b_1(\Phi_{Ly}) = 1.448$)



(a) Behavior of the two degrees of freedom of the section, varying the parameter $a_1(\Phi_{Ly})$



(b) Behavior of the two degrees of freedom of the section, varying the parameter $b_1(\Phi_{Ly})$

Fig. 8 (a) Behavior of the two degrees of freedom of the section, varying the parameter $a_1(\Phi_{Ly})$ and (b) Behavior of the two degrees of freedom of the section, varying the parameter $b_1(\Phi_{Ly})$

oscillation. As the a_1 coefficient grows, the amplitude of the vertical displacements y decreases, in the same manner as the amplitude of motion increases as the b_1 coefficient grows, that is almost linearly.

Relative errors are calculated, observing that a 10% variation of a_1 and b_1 coefficients provides, respectively, a 15% and a 10% variation in the ratio y/y_{max} , while effects decrease to 7% and 9% in the case of α/α_{max} .

In addition, a spectral analysis of the system is performed, to compare the frequency components being involved in the motion with different sets of parameters. The natural frequencies are clearly identified, evidencing but slight differences for variation of a_1 and b_1 coefficients. Spectral analyses performed with different values of the a_1 parameter are shown in Fig. 9.

The function Φ_{My} is described by means of three exponentials, with the pairs of coefficients (a_2, b_2) , (a_3, b_3) and (a_4, b_4) . The effect of this function on the amplitude is very small.

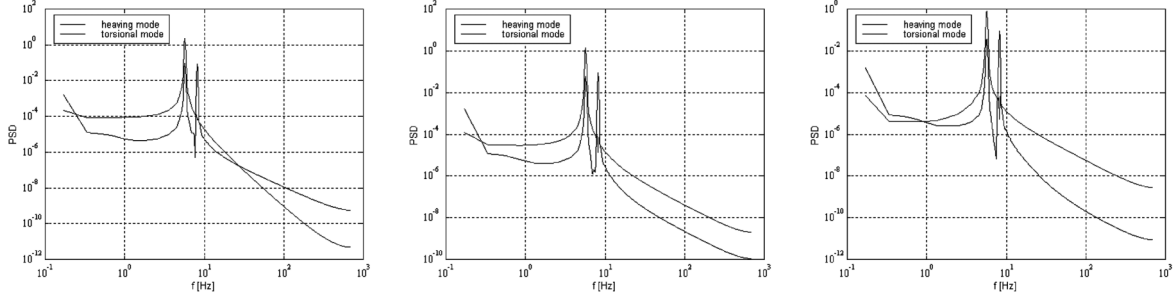


Fig. 9 PSD analysis ($1-a_1(\Phi_{Ly}) = 2.732$, $2-a_1(\Phi_{Ly}) = 3.035$, $3-a_1(\Phi_{Ly}) = 3.339$)

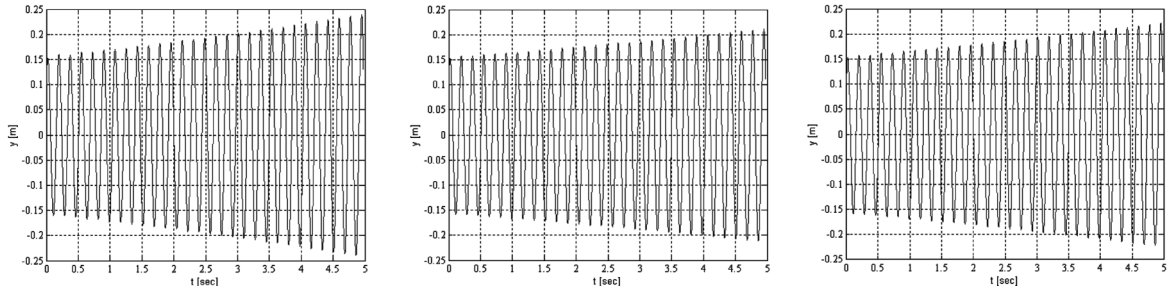


Fig. 10 y displacement vs time: $1-\Phi_{My} (a_2, b_2)$, $2-\Phi_{My} ((a_2, b_2), (a_3, b_3))$, $3-\Phi_{My} ((a_2, b_2), (a_3, b_3), (a_4, b_4))$

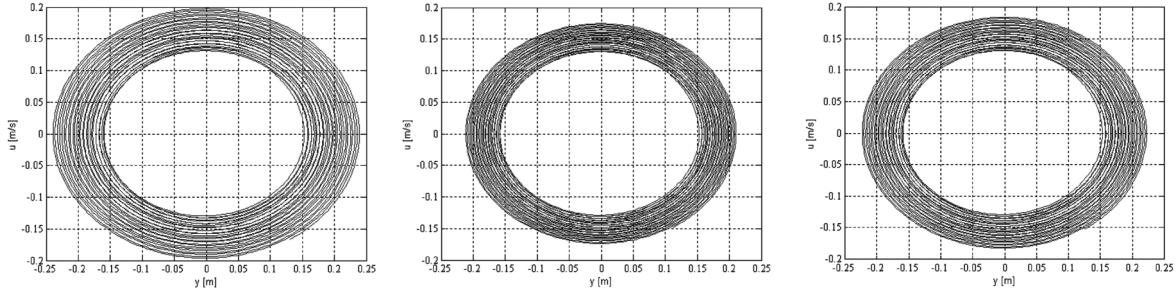
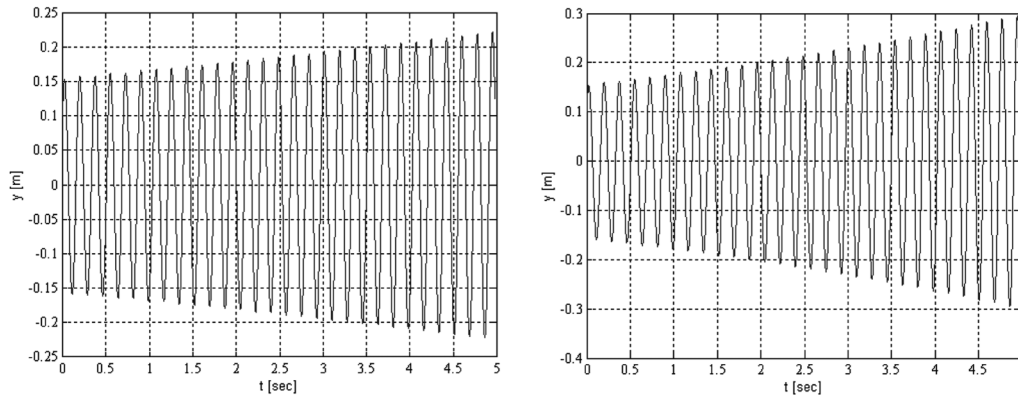


Fig. 11 y displacement vs u : $1-\Phi_{My} (a_2, b_2)$, $2-\Phi_{My} ((a_2, b_2), (a_3, b_3))$, $3-\Phi_{My} ((a_2, b_2), (a_3, b_3), (a_4, b_4))$

An interesting comparison concerns results obtained by means of simplified expressions of Φ_{My} , with only one (a_2, b_2) or two exponential groups $((a_2, b_2)$ and $(a_3, b_3))$. The oscillation amplitude is clearly influenced by a different expression of the function. As an example, time domain plot and phase portrait of the vertical displacement are shown (Fig. 10 and Fig. 11).

The functions related to the variation of the angle of attack $\Phi_{L\alpha}$ and $\Phi_{M\alpha}$ are still described by means of one exponential group, respectively with the pairs of coefficients (a_5, b_5) and (a_6, b_6) . The effect of the variation of coefficients is negligible on the oscillation amplitude and similar to the effect due to variation in Φ_{My} .

Fig. 12 Time history of the y displacement

5.2.2. Limit cases

Parallel analyses are performed to evaluate the behavior of the cross-section with different type of indicial loads, considering the limit cases obtained setting to zero the unsteady contributions, that is the exponentials. Also in this case, the prominent action of the Φ_{Ly} function is evident, being the flutter velocity decided by the values of the corresponding coefficients. The aeroelastic vertical damping related to the Φ_{Ly} function has a strong effect on the section dynamics, increasing dramatically the critical threshold. As an example, in Fig. 12, the time history of the vertical displacement is compared for two cases: the first one represents the y displacement calculated with the unsteady contribution of all four indicial functions, while the second one shows the same displacement with the unsteady contribution of the sole Φ_{Ly} function, evaluating as quasi-steady the terms related to the other functions.

6. Conclusions

In this paper an indicial function model to describe aeroelastic wind loads on a cross-section of a bridge is presented and used to perform parametric analyses. A first study is developed in order to evaluate the influence of the coefficients of the indicial functions on the dynamic behavior of a bridge deck cross-section. The influence of such parameters is found to be mainly on the amplitude of the oscillation, and then, as a consequence, on the critical flutter speed. The main influence is recognized in the Φ_{Ly} function, playing its major role in defining the critical threshold, at least in the case of a streamlined section. This aspect is put in evidence also by the examination of limit cases, to characterize the cross-section dynamics by separating an unsteady and a quasi-steady part in the excitation. The main importance of the lift indicial function is confirmed.

This type of analysis can represent an interesting tool to characterize the expected behavior of the section and can be easily extended to different sections and different groups of indicial functions.

Acknowledgements

The research work is ongoing with the financial grant of MIUR (the Italian “Ministero

dell'Istruzione, Università e Ricerca), under the framework of the Research Project of national interest WINDERFUL (PRIN Cofin 2001). The support of the European Cost Action C14 in Urban Civil Engineering is also gratefully acknowledged.

References

- Bisplinghoff, R.L., Ashley, H. and Halfman, R.L. (1996), *Aeroelasticity*, Dover Publications, Inc., New York.
- Boonyapinyo, V., Miyata, T. and Yamada, H. (1999), "Advanced aerodynamic analysis of suspension bridges by state-space approach", *J. Struct. Eng.*, **125**, 1357-1373.
- Borri, C. and Hoeffler, R. (2000), "Aeroelastic wind forces on flexible girders", *Meccanica*, **35**(10), 1-15.
- Borri, C., Costa, C. and Zahlten, W. (2002), "Non-stationary flow forces for the numerical simulation of aeroelastic instability of bridge decks", *Comp. Struct.*, **80**, 1071-1079.
- Borri, C. and Costa, C. (2004), "Quasi-steady analysis of a bridge deck element", *Comp. Struct.*, **82**, 993-1006.
- Bucher, C.G. and Lin, Y.K. (1989), "Stochastic stability of bridges considering coupled modes", *J. Ind. Aerodyn.*, **91**, 609-636.
- Caracoglia, L. and Jones, N.P. (2003), "Time domain vs. frequency domain characterization of aeroelastic forces for bridge deck sections", *J. Wind Eng. Ind. Aerodyn.*, **91**, 371-402.
- Caracoglia, L. and Jones, N.P. (2003), "A methodology for the experimental extraction of indicial functions for streamlined and bluff deck sections", *J. Wind Eng. Ind. Aerodyn.*, **91**, 609-636.
- Chen, X., Matsumoto, M. and Kareem, A. (2000), "Time domain flutter and buffeting response. Analysis of bridges", *J. Eng. Mech. ASCE*, **126**(1), 7-16.
- Ding, L. and Lee, N.P. (2000), "Computer simulation of buffeting actions of suspension bridges under turbulent wind and bluff deck sections", *Comp. Struct.*, **76**, 609-636.
- Falco, M., Gasparetto, M. and Scaramelli, F. (1978), "Ricerca sul comportamento aeroelastico dei ponti sospesi a grande luce", Technical Report - Politecnico di Milano.
- Fung, Y.C. (1968), *An Introduction to the Theory of Aeroelasticity*, Dover Publications, Inc., New York, 206-216.
- Jones, R.T. (1938), "Operational treatment of the nonuniform-lift theory in airplane dynamics", NACA Report 667, U.S. National Advisory Committee for Aeronautics, Langley, VA, U.S.A.
- Jones, R.T. (1939), *The Unsteady Lift of a Finite Wing*, NACA Report 682, U.S. National Advisory Committee for Aeronautics, Langley, VA, U.S.A.
- Lin, Y.K. and Li, Q.C. (1993), "New stochastic theory for bridge stability in turbulent flow", *J. Eng. Mech.*, **119**(1), 113-127.
- Sarkar, P.P., Jones, N.P. and Scanlan, R.H. (1994), "Identification of aeroelastic parameters of flexible bridges", *J. Eng. Mech. ASCE*, **120**(8), 1718-1742.
- Scanlan, R.H. and Tomko, J.J. (1971), "Airfoil and bridge deck flutter derivatives", *J. Eng. Mech. ASCE*, **97**, 1717-1737.
- Scanlan, R.H., Béliveau, J. and Budlong, K.S. (1974), "Indicial aerodynamic functions for bridge decks", *J. Eng. Mech. Div. ASCE*, **100-EM4**, 657-670.
- Scanlan, R.H. (2000), "Motion-related body-force functions in two-dimensional low-speed flow", *J. Fl. Struct.*, **14**, 49-63.
- Wagner, H. (1925), "Über die Entstehung des dynamischen Auftriebes von Tagflügeln", *Z. Angew. Math. Mech.*, Bd. 5-Helft 1.
- Zhang, X., Brownjohn, J.M.W. and Omenzetter, P. (2003), "Time domain formulation of self-excited forces on bridge deck for wind tunnel experiment", *J. Wind Eng. Ind. Aerodyn.*, **91**, 723-736.